




# Attenuating CD3 affinity in a PSMAxCD3 bispecific antibody enables killing of prostate tumor cells with reduced cytokine release

Kevin Dang <sup>1</sup>, Giulia Castello <sup>1</sup>, Starlynn C Clarke,<sup>1</sup> Yuping Li,<sup>1</sup> Aarti Balasubramani,<sup>1</sup> Andrew Boudreau,<sup>1</sup> Laura Davison,<sup>1</sup> Katherine E Harris,<sup>1</sup> Duy Pham,<sup>1</sup> Preethi Sankaran,<sup>1</sup> Harshad S Ugamraj,<sup>1</sup> Rong Deng,<sup>1</sup> Serena Kwek,<sup>2</sup> Alec Starzinski,<sup>2</sup> Suhasini Iyer,<sup>1</sup> Wim van Schooten,<sup>1</sup> Ute Schellenberger,<sup>1</sup> Wenchao Sun,<sup>1</sup> Nathan D Trinklein,<sup>1</sup> Roland Buelow,<sup>1</sup> Ben Buelow,<sup>1</sup> Lawrence Fong,<sup>2</sup> Pranjali Dalvi <sup>1</sup>

**To cite:** Dang K, Castello G, Clarke SC, *et al.* Attenuating CD3 affinity in a PSMAxCD3 bispecific antibody enables killing of prostate tumor cells with reduced cytokine release. *Journal for ImmunoTherapy of Cancer* 2021;**9**:e002488. doi:10.1136/jitc-2021-002488

► Additional supplemental material is published online only. To view, please visit the journal online (<http://dx.doi.org/10.1136/jitc-2021-002488>).

Accepted 29 April 2021



© Author(s) (or their employer(s)) 2021. Re-use permitted under CC BY-NC. No commercial re-use. See rights and permissions. Published by BMJ.

<sup>1</sup>Teneobio, Inc, Newark, California, USA

<sup>2</sup>Department of Medicine, Division of Hematology/Oncology, University of California San Francisco, San Francisco, California, USA

## Correspondence to

Dr Pranjali Dalvi;  
pdalvi@teneobio.com

## ABSTRACT

**Background** Therapeutic options currently available for metastatic castration-resistant prostate cancer (mCRPC) do not extend median overall survival >6 months. Therefore, the development of novel and effective therapies for mCRPC represents an urgent medical need. T cell engagers (TCEs) have emerged as a promising approach for the treatment of mCRPC due to their targeted mechanism of action. However, challenges remain in the clinic due to the limited efficacy of TCEs observed thus far in solid tumors as well as the toxicities associated with cytokine release syndrome (CRS) due to the usage of high-affinity anti-CD3 moieties such as OKT3.

**Methods** Using genetically engineered transgenic rats (UniRat and OmniFlic) that express fully human IgG antibodies together with an NGS-based antibody discovery pipeline, we developed TNB-585, an anti-CD3xPSMA TCE for the treatment of mCRPC. TNB-585 pairs a tumor-targeting anti-PSMA arm together with a unique, low-affinity anti-CD3 arm in bispecific format. We tested TNB-585 in T cell-redirection cytotoxicity assays against PSMA<sup>+</sup> tumor cells in both two-dimensional (2D) cultures and three-dimensional (3D) spheroids as well as against patient-derived prostate tumor cells. Cytokines were measured in culture supernatants to assess the ability of TNB-585 to induce tumor killing with low cytokine release. TNB-585-mediated T cell activation, proliferation, and cytotoxic granule formation were measured to investigate the mechanism of action. Additionally, TNB-585 efficacy was evaluated *in vivo* against C4-2 tumor-bearing NCG mice.

**Results** *In vitro*, TNB-585 induced activation and proliferation of human T cells resulting in the killing of PSMA<sup>+</sup> prostate tumor cells in both 2D cultures and 3D spheroids with minimal cytokine release and reduced regulatory T cell activation compared with a positive control antibody that contains the same anti-PSMA arm but a higher affinity anti-CD3 arm (comparable with OKT3). *In addition*, TNB-585 demonstrated potent efficacy against patient-derived prostate tumors *ex vivo* and induced immune cell infiltration and dose-dependent tumor regression *in vivo*.

**Conclusions** Our data suggest that TNB-585, with its low-affinity anti-CD3, may be efficacious while inducing a lower incidence and severity of CRS in patients with prostate cancer compared with TCEs that incorporate high-affinity anti-CD3 domains.

## INTRODUCTION

Prostate cancer (CaP) is the second most common cancer in men and the fifth leading cause of cancer death worldwide.<sup>1</sup> It is estimated that there will be 191 930 new cases and 33 330 deaths from CaP in the USA in 2020.<sup>2</sup> Although CaP is usually localized at presentation, it may progress to metastatic disease, which is a major cause of death in patients with advanced CaP.<sup>3</sup> Androgen deprivation therapy in disseminated CaP is the first-line therapy, but patients invariably progress to metastatic castration-resistant prostate cancer (mCRPC).<sup>4</sup> Therapeutic options currently available for mCRPC include non-steroidal antiandrogens (abiraterone and enzalutamide), chemotherapy (docetaxel and cabazitaxel) and sipuleucel-T, but none extend median overall survival >6 months.<sup>5</sup> Thus, novel therapies for the treatment of mCRPC represent an urgent, unmet medical need.

In CaP, tumor cells express a number of prostate-specific surface proteins that represent promising targets for therapy including PSMA, a type II transmembrane protein expressed predominantly on prostate cells.<sup>6–8</sup> PSMA is an attractive target due to its low expression on non-prostatic tissue and its overexpression in a majority of CaP tumors, with expression level correlated to tumor stage and aggressiveness.<sup>9–13</sup> The overexpression of PSMA in CaP has been shown to



promote tumor progression through the aberrant activation of PI3K-AKT signaling pathways.<sup>14</sup> Therefore, a diverse array of PSMA-targeted therapies are in development including radionuclides, antibody drug conjugates, chimeric antigen receptor T cells and T cell engagers (TCEs).<sup>15</sup>

TCEs are heterodimeric antibodies engineered to simultaneously bind to a tumor-associated antigen on cancer cells and to CD3 on T cells, forming an immunological synapse that promotes T cell redirected lysis of tumor cells in an MHC-independent manner.<sup>16</sup> Although T cell redirection is promising, all such approaches to date induce strong pan-T cell stimulation and toxic immune activation culminating in the systemic release of proinflammatory cytokines leading to cytokine release syndrome (CRS). This major side effect of TCE therapy can potentially be attributed to the fact that a majority of TCEs developed thus far incorporate strong binding/activating anti-CD3 moieties with affinities in the 1–200 nM range such as OKT3 and UCHT1.<sup>17</sup> Despite their effectiveness in hematologic tumors, TCEs have also demonstrated limited success in solid tumors, and combination treatments may be needed to maximize efficacy.<sup>18,19</sup>

Currently, a number of TCEs targeting PSMA and CD3 are being investigated in early phase clinical studies for the treatment of mCRPC. Pasotuzumab (AMG 212), a PSMA-targeting bispecific T cell engager (BiTE), demonstrated signs of clinical activity in a phase I study as approximately one-third of patients in the 20, 40, and 80 µg/dose groups of the continuous intravenous infusion (cIV) cohort exhibited a >50% decline in Prostate-specific antigen (PSA) levels.<sup>20</sup> Due to a sponsor change, this study was terminated early, and the maximum tolerated dose for the cIV cohort was not determined. AMG 160 is a half-life extended BiTE also being investigated in phase I clinical trials. In contrast to the high-frequency, once-daily dosing regimen of pasotuzumab, AMG 160 is administered once every 2 weeks. Data from the phase I study indicate that 27.6% of patients had a confirmed PSA response to AMG 160, although grade 2 and grade 3 CRS occurred in 60.5% and 25.6% of patients, respectively.<sup>21</sup> For HPN424, a once-weekly dosed TriTAC molecule targeting PSMA and CD3, clinical activity at the highest fixed dose tested (160 ng/kg) was demonstrated by PSA reduction in three out of seven patients with one confirmed partial response.<sup>22</sup> Overall, these phase I clinical trial data suggest that, although promising, there are shortcomings associated with current PSMA-targeted TCE therapeutics, including either safety (polycytokine secretion and clinical CRS), efficacy, or dosing schedule, that could be addressed by an IgG TCE that facilitates tumor killing with minimal cytokine release.

Given that T cells possess a dual activation threshold (one for cytotoxicity and the other for cytokine production)<sup>23</sup> and that the formation of a stable mature immunological synapse is not required for T cell cytotoxicity,<sup>24</sup> we hypothesized that a low-affinity anti-CD3 more closely resembling the low-affinity interaction of the TCR:pMHC

complex could enable T cell-mediated killing to be uncoupled from cytokine release. Previous work from our lab identified such a low-affinity anti-CD3 (CD3\_F2B), which induced tumor killing with minimal cytokine release against hematologic tumors including multiple myeloma (MM) and B cell non-Hodgkin's lymphoma.<sup>25,26</sup> To extend these favorable properties into the solid tumor setting, we developed TNB-585, a fully human anti-CD3xPSMA IgG4 TCE for the treatment of mCRPC. TNB-585 combines a tumor-targeting anti-PSMA arm together with our low affinity anti-CD3\_F2B to facilitate T cell redirected killing of prostate tumor cells with minimal cytokine release. TNB-585 mediated killing of PSMA<sup>+</sup> tumor cells (two-dimensional (2D) cultures and three-dimensional (3D) spheroids) in vitro and of patient-derived prostate tumors ex vivo. In addition, TNB-585 induced immune cell infiltration and dose-dependent tumor regression in vivo in an NCG mouse xenograft model. Notably, TNB-585 induced substantially lower cytokine production and regulatory T cell (Treg) activation while maintaining equivalent levels of maximum tumor killing compared with a positive control antibody that contains the same anti-PSMA arm but a higher affinity anti-CD3 arm. With potent antitumor activity combined with a favorable safety profile, TNB-585 will potentially create a safer and more effective therapy for mCRPC and expand the opportunities for its use in combination treatments.

## MATERIALS AND METHODS

### Immunization, NGS, clonotype analysis, and cloning

Using genetically engineered transgenic rats (UniRat and OmniFlic) that express fully human IgG antibodies together with an NGS-based antibody discovery pipeline (TeneoSeek),<sup>25–28</sup> we have developed TNB-585. Methods for generating antibodies targeting CD3 in OmniFlic animals have been previously described.<sup>25</sup> For generating heavy chain only antibodies against PSMA, 12 UniRats were immunized with recombinant human PSMA protein fused to a his-tag (R&D Systems, Minneapolis, Minnesota, USA) for up to 8 weeks using either Titermax/Ribi or CFA/IFA adjuvant. Draining lymph nodes from all animals were then harvested, and total RNA was collected. cDNA samples containing the full heavy chain variable domain (VH) underwent next-generation sequencing using the MiSeq platform (Illumina, San Diego, California, USA) with 2×300 paired-end reads. Data from all animals were analyzed, and the most frequent 265 VH sequences were selected for cloning followed by expression in HEK 293 cells.

### Expression and purification of TNB-585, positive control (PC), and negative control (NC) TCEs

TNB-585 consists of two heavy and one light chain(s) paired using knobs-into-holes technology.<sup>29,30</sup> Heavy chain 1 (HC1) and the kappa light chain form the paratope that binds to human CD3. Heavy chain 2 (HC2) is composed of a single VH domain that targets PSMA. The

Fc contains a mutation that results in the loss of Fc-mediated effector functions in order to disable non-specific activation and depletion of T cells in patients. TNB-585 is further engineered to prevent arm-exchange with other IgG4 molecules.

The positive control (PC) antibody is composed of an HC2 (anti-PSMA) and Fc region identical to TNB-585, whereas the heavy chain and the kappa light chain on the other arm combine to form a paratope that binds to human CD3 with stronger affinity than TNB-585. The affinity of the CD3 arm in the PC is similar to OKT3 (muronomab-CD3). The NC antibody is composed of an HC1 (anti-CD3) and an Fc region identical to TNB-585. However, the VH domain on the targeting arm of the NC is against an irrelevant, non-human target.

TNB-585, PC, and NC antibodies were expressed in ExpiCHO cells as per manufacturer's instructions. Supernatants were harvested, clarified, and affinity purified using an anti-CH1 resin (CaptureSelect CH1-XL, ThermoFisher, Waltham, Massachusetts, USA), followed by a polishing step with size exclusion or cation exchange chromatography.

#### SDS-PAGE and capillary gel electrophoresis

Purified proteins were run on a 4%–12% Bis-Tris SDS-PAGE gel (NuPAGE, ThermoFisher) under non-reducing conditions, followed by Coomassie Blue staining. Analysis was performed on Image Lab (Bio-Rad Laboratories, Hercules, California, USA) against a prestained protein ladder (PageRuler, ThermoFisher) run on the same gel. Capillary gel electrophoresis was performed on Maurice (ProteinSimple, San Jose, California, USA) using its preassembled, prequalified CE-SDS cartridge. Purified proteins were mixed with internal standard (ProteinSimple) and iodoacetamide according to manufacturer's instructions, denatured at 70°C for 10 min, and separated by electrophoresis for 35 min at 5750V.

#### Size exclusion ultra-performance liquid chromatography (UPLC)

Size exclusion UPLC was performed on a ThermoFisher Ultimate 3000 UPLC with a UV/Vis detector set to 280 nm and 220 nm for monitoring. The SEC column (TSKgel UP-SW3000, 2 µm, 30 cm × 4.6 mm) was from Tosoh Bioscience. The isocratic method was run in 100 mM Sodium Citrate, 500 mM Sodium Chloride, 200 mM L-Arginine, pH 6.2 at a flow rate of 0.25 mL/min.

#### Potency assay

Determination of TNB-585 potency before and after heat stress was evaluated using a T cell activation bioassay (Promega, Madison, Wisconsin, USA). In brief, 22Rv1 cells were seeded in 96-well tissue culture plates and incubated overnight at 37°C. Following incubation, culture supernatant was aspirated and replenished with assay media (RPMI 1640, 10% fetal bovine serum (FBS)) along with a dilution series of antibody. TCR/CD3 effector cells were then thawed, resuspended in assay media, and added

to each well. After a 6-hour incubation at 37°C, Bio-Glo reagent was added to each well, and luminescence was measured on a SpectraMax i3x microplate reader (Molecular Devices, San Jose, California, USA).

#### Assessment of pharmacokinetics in cynomolgus monkey

Nine male cynomolgus monkeys were administered a single intravenous bolus dose of 0.07, 0.97, or 10.39 mg/kg TNB-585 (Alta Science Preclinical Seattle, Everett, Washington, USA). Blood samples collected from a peripheral vein were processed to serum on day -12 (predose), and on days 1 (1 hour and 6 hours postdose), 2, 3, 5, 7, 15 and 21. Concentrations of TNB-585 in serum were measured by ELISA. In brief, a rabbit anti-idiotypic antibody against the anti-PSMA arm was coated at 1 µg/mL onto 96-well plates and incubated overnight at 4°C. The plates were then washed three times with wash buffer (TBST +0.1% Tween-20) and blocked using 1% milk for 1 hour at room temperature. Following incubation, the plates were washed, and 100 µL of diluted serum was added to each well and incubated for 2 hours at room temperature. After three washes, a rat anti-idiotypic antibody against the anti-CD3 arm was added at 1 µg/mL for 30 min. Binding was detected by incubation with anti-rat IgG2a-HRP followed by addition of ELISA Ultra TMB substrate. After sufficient color developed, 100 µL of stop solution was added to each well. Absorbance was read at 450 nm on a SpectraMax i3x plate reader. TNB-585 concentrations in serum were determined by interpolation from the standard curve. Non-compartmental PK parameters were estimated using Phoenix WinNonlin V.8.1 software (Certara USA, Inc, Princeton, New Jersey, USA).

#### Cell lines and cell culture

Prostate tumor cell lines LNCaP, 22Rv1, MDA-PCa-2b, PC3, and DU145 were purchased from ATCC (Manassas, Virginia, USA). LNCaP and 22Rv1 cells were cultured in RPMI-1640 (Fisher Scientific, Waltham, Massachusetts, USA) and 10% FBS (ThermoFisher). DU145 cells were cultured in EMEM (ATCC) and 10% FBS. PC3 cells were cultured in F12K (ATCC) and 10% FBS. MDA-PCa-2b cells were cultured in BRFF-HPC1 (Athena Enzyme Systems, Baltimore Maryland, USA) and 20% FBS. All cell lines were maintained in a humidified chamber at 37°C and 8% CO<sub>2</sub>.

A stable PSMA-overexpressing PC3 cell line (PC3-PSMA) was developed at Antibody Solutions (Santa Clara, California, USA). PSMA cDNA was synthesized and cloned into a stable integration expression vector and transfected into PC3 cells using Lipofectamine 3000 (ThermoFisher). Cells transiently expressing the transfected DNA were selected using puromycin to generate stable expressing pools. High-expressing clones were then isolated by fluorescence-activated cell sorting. PSMA cells were cultured in F12K with 10% FBS and 1 µg/mL puromycin (ThermoFisher).

### Cell binding and flow cytometry

Binding of TNB-585 to PSMA<sup>+</sup> and PSMA<sup>-</sup> cells was evaluated by flow cytometry. In brief, tumor cells were incubated with a dilution series of antibody for 30 min at 4°C. After incubation, the cells were washed twice with flow cytometry buffer (PBS, 1% BSA, 0.1% NaN<sub>3</sub>), resuspended in a 1:100 diluted solution of PE-conjugated goat antihuman IgG secondary antibody (Southern Biotech, Birmingham, Alabama, USA), and incubated for 20 min at 4°C. The cells were then washed twice in flow cytometry buffer, and the mean fluorescence intensity (MFI) was measured using either FACSCelesta (BD Biosciences, San Jose, California, USA) or Guava easyCyte 8HT (EMD Millipore, Hayward, California, USA).

To determine PSMA antigen density, the cells were stained with a saturating concentration of PE-conjugated anti-PSMA antibody (BioLegend, San Diego, California, USA), and the MFI was measured by flow cytometry. A calibration curve was generated using BD Quantibrite Beads (BD Biosciences), which are composed of distinct bead populations containing a known number of molecules of equivalent fluorochrome (MESF) to convert the MFI of a sample to the number of PE molecules on the cell surface. A linear regression of log<sub>10</sub>(MESF) against log<sub>10</sub>(MFI) was plotted to calculate the number of antibodies bound per cell (ABC) using a PE to mAb ratio of 1:1. The ABC was then multiplied by two to approximate the antigen density assuming that, at saturation, one antibody binds to two antigen molecules.

### Cytotoxicity and cytokine analysis

Prostate tumor cells were labeled with 0.5 μM 1'-dioctadecyl-3,3,3',3'-tetramethylindotricarbocyanine iodide (DiR', ThermoFisher), as per manufacturer's instructions, and incubated with human T cells at an effector to target (E:T) ratio of 10:1 in the presence antibody for 48–72 hour at 37°C and 8% CO<sub>2</sub>. To measure tumor killing, the cells were stained with FITC-conjugated Annexin-V (BioLegend) and analyzed by flow cytometry. Alternatively, the cells were incubated with a 1:10 dilution of WST-1 for 90 min at 37°C, and absorbance was measured at 450 nm using a SpectraMax i3x microplate reader to colorimetrically assess cell viability.

For cytokine analysis, culture supernatant was harvested at 48 or 72 hours and used to quantify cytokines by ELISA (BioLegend) or Meso Scale Discovery technology (Meso Scale Diagnostics, Rockville, Maryland, USA) as per manufacturer's instructions.

### Granzyme and perforin analysis

LNCaP cells (15,000 cells/well) were incubated with human T cells at an E:T ratio of 10:1 in the presence of antibody for 48 hours at 37°C and 8% CO<sub>2</sub>. Following incubation, culture supernatants were harvested, and granzyme and perforin concentrations were determined using human granzyme B ELISA (ThermoFisher) and human perforin ELISA (Cell Sciences, Newburyport, Massachusetts, USA).

### Measurement of T cell proliferation

22Rv1 and DU145 cells were seeded (25,000 cells/well) in a 96-well plate and incubated overnight at 37°C and 8% CO<sub>2</sub>. Following incubation, human T cells were labeled with 2 μM carboxyfluorescein succinimidyl ester (CFSE, ThermoFisher), as per manufacturer's instructions, and co-cultured with tumor cells at an E:T ratio of 4:1 in the presence of antibody for 48 hours at 37°C and 8% CO<sub>2</sub>. The cells were then stained with fluorophore conjugated anti-CD4 and anti-CD8 antibodies (BioLegend) and analyzed by flow cytometry. Proliferation was calculated as the percent of T cells that showed a reduction in CFSE signal compared with untreated control.

### Measurement of CD4, CD8, and regulatory T cell activation

LNCaP and DU145 cells were seeded (20,000 cells/well) in a 96-well plate and incubated overnight at 37°C and 8% CO<sub>2</sub>, followed by incubation with human T cells at an E:T of 5:1 in the presence of antibody for 48 hours at 37°C and 8% CO<sub>2</sub>. The cells were then stained with fluorophore-conjugated antibodies against CD4, CD8, CD69, CD25, and Foxp3 and analyzed by flow cytometry. Activation was measured by the upregulation of CD69, a marker of T cell activation. The percentage of Tregs within the activated T cell population (CD69<sup>+</sup>) was determined by sub-gating on CD25<sup>+</sup> and Foxp3<sup>+</sup> cells.

### Evaluation of TNB-585 efficacy in 3D tumor spheroid models

Ninety-six well round-bottom, non-treated microplates (Corning, Barrington, New Jersey, USA) were coated with antiadherence solution (STEMCELL Technologies, Kent, Washington, USA), centrifuged for 5 min at 500× g and washed once with spheroid growth media (RPMI-1640 containing 10% FBS). LNCaP cells were seeded (5000 cells/well) and incubated at 37°C and 8% CO<sub>2</sub>. Half of the media was replenished with fresh media every 2 days. On day 7, antibody was added to each well together with healthy donor PBMCs at an E:T of 1:1. Images were taken daily using a Nikon TMS inverted phase-contrast microscope connected to a 16MP digital camera (Boli-Optics, Rancho Cucamonga, California, USA) to capture morphological changes in the spheroid. After 4 days of antibody treatment, culture supernatant was harvested to measure Interleukin-2 (IL-2), interferon gamma (IFNγ), and tumor necrosis factor alpha (TNFα) by MSD. Tumor killing was determined using CytoTox 96 Non-Radioactive Cytotoxicity Assay (Promega) per manufacturer's instructions. Percent cytotoxicity was determined using the formula  $[(OD_{test} - OD_{no\ antibody\ control}) / OD_{test}] \times 100$ . To qualitatively evaluate cytotoxicity, the spheroids were stained with trypan blue after 4 days of treatment followed by microscopic imaging at 4× magnification.

### Immunohistochemical staining of spheroids

Immunohistochemical staining of the spheroids was performed to evaluate T cell infiltration. Histology, IHC staining, and whole slide scanning were performed by NDB Bio, LLC (Baltimore, Maryland, USA). In brief,

the spheroids were paraformaldehyde fixed, embedded in Histogel, dehydrated in gradient concentrations of ethanol, cleared in xylene, and embedded in paraffin wax. Sections 4  $\mu\text{m}$  thick were stained with antibodies against PSMA (Clone 3E6; Dako) and CD8 (Clone C8/144B; Cell Marque). Whole slide scans were generated using an Olympus PlanN 20 $\times$  objective (N.A. 0.40). Scans were viewed and analyzed using ImageScopeX64 software.

### Ex vivo processing of patient prostate tumors

Tumor cells were either isolated from fresh prostate tumor tissue procured from LF's lab at UCSF (San Francisco, California, USA) or received as frozen dissociated aliquots along with donor matched PBMCs from Discovery Life Sciences (Newtown, Pennsylvania, USA). The fresh prostate tissue was dissociated as previously described.<sup>31</sup> For the cytotoxicity assay, exogenous human PBMCs were co-cultured with dissociated tumor cells at an E:T of 1:2 for 24 hours at 37°C, 8% CO<sub>2</sub>. The death of PSMA<sup>+</sup> cells was analyzed by flow cytometry on the BD FACSCelesta. An anti-CD45 antibody (BioLegend) was used to distinguish hematopoietic cells, and a non-epitope competing anti-PSMA antibody (clone LNI17, BioLegend) was used to identify PSMA<sup>+</sup> cells. The percentage of PSMA<sup>+</sup> live cells was determined using eBioscience Fixable Viability Dye eFluor 780 (Invitrogen, Carlsbad, California, USA). Culture supernatant from each well was used to measure IL-2, IFN $\gamma$ , and TNF $\alpha$  by MSD.

### In vivo assessment of TNB-585 in an NCG mouse xenograft model

In vivo antitumor activity of TNB-585 was evaluated in murine models of CaP (Crown Bioscience, Taicang, China). In the first study, immunodeficient NCG mice (n=3) were engrafted subcutaneously with 2 $\times$ 10<sup>6</sup> C4-2 tumor cells followed by implantation of 10 $\times$ 10<sup>6</sup> of either resting pan-T cells or preactivated PBMCs 1 day post-engraftment. PBMCs were activated 3 days prior to implantation by incubation with anti-CD28 in tissue culture plates coated with anti-CD3 (both at 1  $\mu\text{g}/\text{mL}$ ). Treatment began 9 days post-tumor engraftment when the average tumor volume was  $\sim$ 50 mm<sup>3</sup>. Mice were randomized into groups and received treatment of TNB-585, PC, or NC (150  $\mu\text{g}/\text{dose}$ ) antibody via tail vein injection twice per week for a total of five doses. Tumor burden was monitored biweekly, and the study was terminated when the tumor volumes in the control group exceeded 2000 mm<sup>3</sup>. After termination of the in-life portion of the study, the tumors were harvested, processed into formalin-fixed paraffin-embedded sections, and stained using an anti-human CD45 antibody following a standard protocol to visualize immune cell infiltration into the tumor. The stained sections were scanned with NanoZoomer-HT 2.0 Image system (Hamamatsu, Japan) for 40 $\times$  magnification, and the images were analyzed using the HALO platform (Indica Labs, Albuquerque, New Mexico, USA).

In a follow-on study, six cohorts of immunodeficient NCG mice (n=4) were engrafted subcutaneously with

2 $\times$ 10<sup>6</sup> C4-2 tumor cells. One day postimplantation, 10 $\times$ 10<sup>6</sup> preactivated human PBMCs were administered intraperitoneally. Treatment began 6 days post-tumor engraftment when the average tumor size was  $\sim$ 50 mm<sup>3</sup>. Mice were randomized into groups and received TNB-585 treatment (5.5, 16.6, 50, 150, or 450  $\mu\text{g}$  per dose) via tail vein injection twice per week for a total of 8 treatments. Tumor burden was monitored biweekly, and the study was terminated when the volumes in the control group exceeded 1000 mm<sup>3</sup>. The tumors were then harvested and stained using an antihuman CD45 antibody to assess immune cell infiltration into the tumor.

### Statistics

Statistical analysis was performed using one-way analysis of variance (ANOVA) with a post hoc Tukey's test for multiple comparisons. Two-sided p values were calculated for all in vitro experiments using GraphPad Prism V.8. The results were judged statistically significant when the Bartlett's corrected p values were less than 0.05. A non-parametric Mann-Whitney test at a significance level of 0.05 was used for the assays containing only two data sets. Data from in vivo studies were analyzed in R language (V.3.3.1) using one-way ANOVA.

## RESULTS

### Discovery of TNB-585, a PSMA $\times$ CD3 bispecific antibody

Discovery and characterization of lead anti-CD3 antibodies have been previously described.<sup>25</sup> To generate lead anti-PSMA antibodies, 265 heavy chain only antibodies (UniAbs) identified using a custom NGS-based approach on immunized UniRats were selected for gene assembly, recombinant expression, and functional screening. High-throughput ELISA and cell binding screens identified 40 PSMA-specific binders from 12 different CDR3 clonotype families. An additional 117 VH sequences were identified by antibody repertoire analysis of four lead CDR3 clonotype families that contain sequence variation in CDR1, CDR2, and framework regions. Candidates were assessed for cell binding to PSMA<sup>+</sup> cell lines, and the top binders from each CDR3 family were scaled up for further studies. To identify high-affinity anti-PSMA leads, cell binding dose curves were performed with LNCaP cells, and the dissociation constants were determined by biolayer interferometry using an Octet QK384. High-affinity anti-PSMA leads were combined into TCEs using knobs-into-holes technology with our previously identified low-affinity anti-CD3\_F2B arm that mediates tumor killing with minimal cytokine secretion. The TCEs were evaluated in parallel for their functional characteristics, including cytotoxicity and cytokine release, as well as their developability characteristics. A final lead TCEs was selected and designated TNB-585.

### TNB-585 is a stable molecule with favorable developability characteristics

TNB-585 is stable at 4°C and 37°C as represented by a single band and a single peak on SDS-PAGE and

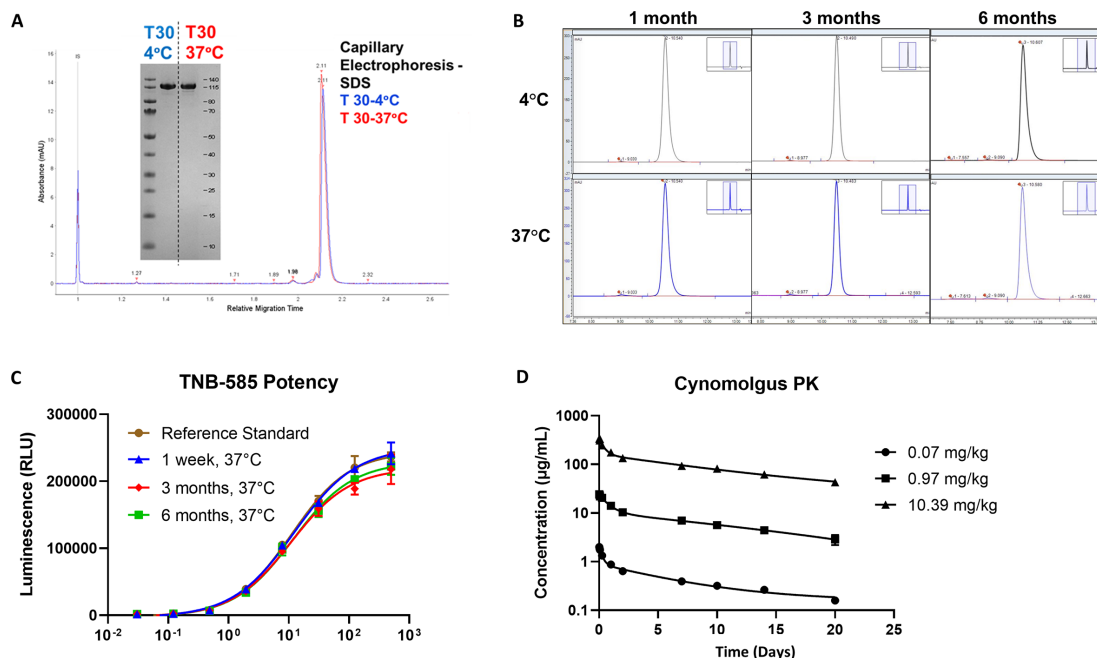


**Figure 1** TNB-585 is a stable molecule with favorable developability characteristics. (A) TNB-585 stability was assessed following incubation at 37°C for 1 month. High and low molecular weight species were analyzed by CE-SDS and SDS-PAGE. (B) SE-UPLC chromatograms of TNB-585 stressed at 37°C for 1, 3, and 6 months compared with 4°C are shown. (C) TNB-585 activity was measured using a T cell activation bioassay after heat stress at 37°C at 1 week, 3 months, and 6 months. (D) PK in cynomolgus monkeys was evaluated by ELISA following a single dose intravenous administration of TNB-585 at 0.07, 0.97, or 10.39 mg/kg.

capillary electrophoresis, respectively (figure 1A). After incubation at 37°C for 1, 3, and 6 months, no significant increase in high molecular weight species was observed by SEC-UPLC (figure 1B). Similarly, TNB-585 maintained potency after heat stress, as demonstrated in a T cell activation bioassay (figure 1C). Relative potencies are listed in table 1. TNB-585 was also assessed in a single-dose Pharmacokinetics (PK) study in cynomolgus monkey. Group mean serum concentrations versus time profiles are shown in figure 1D. Group mean PK parameter estimates are provided in table 2. TNB-585 PK was linear across the dose range of 0.1–10 mg/kg (nominal dose, actual doses were 0.07–10.39 mg/kg). Group mean CL ranged from 4.16 to 6.78 mL/day/kg and group mean  $t_{1/2}$  ranged from 9.75 to 11.0 days following single intravenous doses ranging from 0.1 to 10 mg/kg in cynomolgus monkeys. Since TNB-585 does not cross-react with CD3 or PSMA in non-human primates, the observed linear PK is consistent with non-specific clearance mechanisms dominating PK. The PK profiles

observed in cynomolgus monkeys were consistent with that of an IgG with linear PK, indicating stability of TNB-585 in serum *in vivo*.

### TNB-585 binds to PSMA and CD3 and induces antigen-dependent cytotoxicity and cytokine release

Specific binding of TNB-585 to PSMA was confirmed by flow cytometry on various PSMA<sup>+</sup> and PSMA<sup>-</sup> cell lines (figure 2A). TNB-585 demonstrated dose-dependent binding to PSMA<sup>+</sup> cells with EC<sub>50</sub> values ranging from 24.1 nM to 38.4 nM (table 3). No binding of TNB-585 to PSMA<sup>-</sup> cells was observed. To evaluate high, medium, and low PSMA-expressing cell lines, the antigen densities were determined by flow cytometry using fluorescent beads that allow for the conversion of MFI to the number of antigen molecules on the surface of the cell. As shown in table 3, 22Rv1, LNCaP, MDA-PCa-2b, and PC3-PSMA cells expressed a wide range of PSMA antigens on the cell surface. PSMA expression on CaP cell lines such as LNCaP has been demonstrated to be representative of human CaP for preclinical studies.<sup>32</sup> The PC3-PSMA cells, which expressed the highest levels of PSMA, were used to assess initial proof of activity of TNB-585 in comparison with non-transfected, PSMA<sup>-</sup> PC3 cells (PC3-WT). As shown in figure 2B, T cell redirected killing and cytokine release induced by TNB-585 is dependent on PSMA expression. Additionally, we observed TNB-585-mediated cytotoxicity at multiple E:T ratios (online supplemental file S1).

**Table 1** TNB-585 potency after heat stress

TNB-585	EC <sub>50</sub> (nM)	% relative potency
Reference standard	11.2	100
1 week, 37°C	12.3	91
3 months, 37°C	10.9	102
6 months, 37°C	11.9	94

EC<sub>50</sub>, Half maximal effective concentration.

**Table 2** PK parameters of TNB-585 in cynomolgus monkeys

Parameter	Units	0.07 mg/kg		0.97 mg/kg		10.39 mg/kg	
		Mean	SD	Mean	SD	Mean	SD
$C_{max}$	$\mu\text{g/mL}$	2.0	0.1	24.5	1.1	344	39
$C_{max}/D$	$(\mu\text{g/mL})/(\text{mg/kg})$	28.7	1.7	25.3	1.1	33.1	3.8
$t_{1/2}$	Days	9.9	0.7	9.8	3.0	11	1.3
$AUC_{inf}$	$\mu\text{g/mL}\cdot\text{days}$	10.4	0.8	178	48.9	2500	118
$AUC_{inf}/D$	$(\mu\text{g/mL}\cdot\text{days})/(\text{mg/kg})$	148	10.8	184	50.4	241	11.3
% Extrap	%	21.9	1.8	22.6	9.8	27.1	2.7
CL	$\text{mL/day/kg}$	6.8	0.5	5.7	1.6	4.2	0.2
$V_{ss}$	$\text{mL/kg}$	86.8	1.3	72.2	2.6	62.7	2.5

$AUC_{inf}$ : area under the serum concentration-time curve from time zero to infinity;  $AUC_{inf}/D$ , dose-adjusted area under the serum concentration-time curve;  $C_{max}$ : maximum serum drug concentration; CL, serum clearance;  $C_{max}/D$ , dose-adjusted maximum serum drug concentration; % Extrap, area under the serum concentration-time curve extrapolated from time  $t$  to infinity as a percentage of total AUC;  $t_{1/2}$ , half-life;  $V_{ss}$ , apparent volume of distribution at steady state.

### Activation of T cells by TNB-585 induces CD69 upregulation, proliferation, and perforin and granzyme production

To evaluate the mechanism of action of TNB-585, LNCaP (PSMA<sup>+</sup>) or DU145 (PSMA<sup>-</sup>) cells were co-cultured with T cells in the presence of increasing concentrations of TNB-585, PC, or NC and analyzed by flow cytometry to measure the upregulation of CD69, a marker of T cell activation. TNB-585 induced antigen-dependent and dose-dependent activation of T cells comparable with the PC but with reduced potency (figure 3A). The  $EC_{50}$  values for TNB-585 mediated CD4<sup>+</sup> and CD8<sup>+</sup> T cell activation were 27.1 nM and 31.2 nM, respectively, while the maximum percent activation ranged from 53.3% to 67.3%. For the PC, the  $EC_{50}$  of both CD4<sup>+</sup> and CD8<sup>+</sup> T cell activation

was approximately 0.01 nM, while the maximum percent activation ranged from 59.7% to 62.2%. Minimal CD69 upregulation was observed in the presence of DU145 cells or NC.

TNB-585-mediated T cell proliferation was assessed by incubating CFSE-labeled T cells with 22Rv1 (PSMA<sup>+</sup>) or DU145 (PSMA<sup>-</sup>) tumor cells and increasing concentrations of TNB-585, PC, or NC. Following a 5-day incubation, percent proliferation was measured by flow cytometry as the percent of T cells that showed a reduction in CFSE signal compared with untreated control. The dose-response curves in figure 3B demonstrate that TNB-585 induced antigen-dependent and dose-dependent proliferation of CD4<sup>+</sup> and CD8<sup>+</sup> T cells. The  $EC_{50}$  values of

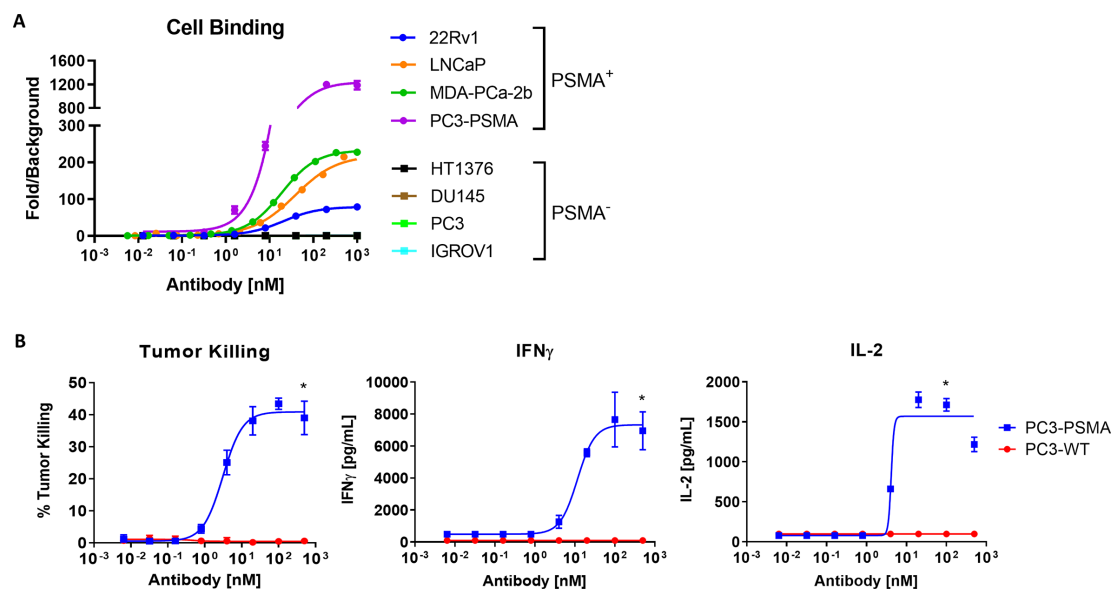


**Figure 2** TNB-585 binds to PSMA and CD3 and induces antigen-dependent cytotoxicity and cytokine release. (A) Dose-response curves of TNB-585 binding to multiple on-target (22Rv1, LNCaP, MDA-PCa-2b and PC3-PSMA) and off-target (HT1376, DU145, PC3 and IGROV-1) cell lines as assessed by flow cytometry are shown. (B) TNB-585-mediated cytotoxicity and cytokine release was evaluated against either PSMA-transfected (PC3-PSMA) or non-transfected (PC3-WT) PC3 tumor cells. Cytotoxicity was evaluated by annexin V staining using flow cytometry. IFN $\gamma$  and IL-2 concentrations were measured by ELISA. Data are reported as mean $\pm$ SD. \* $p < 0.05$  compared with PC3-WT.

**Table 3** PSMA antigen density and  $EC_{50}$  of TNB-585 binding on prostate tumor cell lines

Cell line	Antigen density	$EC_{50}$ (nM)
22Rv1	33,000±60	24.1
LNCaP	170,000±7000	38.4
MDA-PCa-2b	200,000±200	28
PC3-PSMA	951,000±13400	26.8

TNB-585 mediated proliferation were 20.4 nM and 21.84 nM for  $CD4^+$  and  $CD8^+$  T cells, respectively, while the maximum percent proliferation ranged from 70.5% to 87.8%. For the PC, the  $EC_{50}$  of both  $CD4^+$  and  $CD8^+$  T cell proliferation was 0.02 nM, while the maximum percent proliferation ranged from 91.4% to 96.0%. No T cell proliferation was observed in the presence of either DU145 cells or NC, demonstrating target-specificity of TNB-585.

To evaluate the mechanism of T cell mediated cytotoxicity by TNB-585, we analyzed the production of effector molecules released from cytotoxic lymphocytes: the pore-forming protein, perforin, and the serine protease, granzyme. Perforin and granzyme concentrations were measured from LNCaP and T cell co-culture supernatants

after 48 hours of treatment with TNB-585, PC, or NC. As seen in [figure 3C](#), TNB-585 mediated the release of both perforin and granzyme from T cells at levels comparable with the PC. Minimal levels were detected in the NC-treated cells. These data are consistent with the traditional view that the perforin and granzyme pathway is one of the primary mechanisms used by effector T cells to eliminate target cells.<sup>33</sup>

### TNB-585 induces preferential activation of effector T cells over Tregs

Since the mechanism of action of TCEs is T cell redirected killing, overstimulation of Tregs, an immunosuppressive T cell subset, can potentially suppress antitumor immunity. Therefore, the relative ability of TNB-585 to activate  $CD4^+$  and  $CD8^+$  effector T cells versus Tregs was compared with the PC. T cells isolated from three healthy donors were incubated with LNCaP cells and increasing concentrations of TNB-585, PC, or NC for 48 hours. Activation was assessed by measuring CD69 upregulation by flow cytometry. To determine the relative activation of Tregs induced by TNB-585 and the PC, the percentage of Tregs within the activated T cell population ( $CD69^+$ ) was measured by subgating on  $CD25^+Foxp3^+$  cells. While TNB-585 stimulated equivalent levels of maximum T

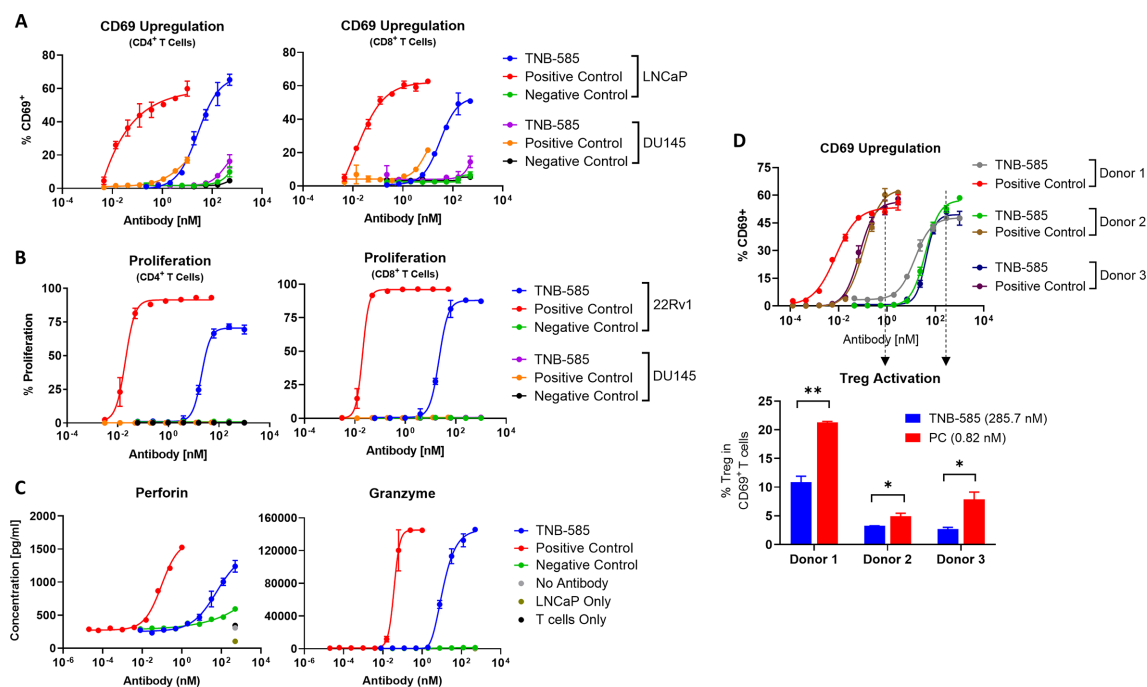


**Figure 3** Activation of T cells by TNB-585 induces CD69 upregulation, proliferation, and perforin and granzyme production. (A) CD69 upregulation was assessed on  $CD4^+$  and  $CD8^+$  T cells by flow cytometry following incubation of LNCaP or DU145 tumor cells and T cells in the presence of increasing concentrations of TNB-585, PC, or NC for 48 hours at 37°C. (B) proliferation of CFSE-labeled  $CD4^+$  and  $CD8^+$  T cells was assessed following incubation with 22RV1 or DU145 tumor cells in the presence of increasing concentrations of TNB-585, PC, or NC for 48 hours at 37°C. Percent proliferation was measured by CFSE dilution using flow cytometry. (C) Perforin and granzyme concentrations in culture supernatants were measured by ELISA after 48 hours incubation of TNB-585, PC, or NC with T cells and LNCaP tumor cells. (D) Upregulation of CD69 on T cells from three healthy donors was measured by flow cytometry after 48 hours incubation with 22RV1 tumor cells and either TNB-585, PC, or NC. Activated T cells ( $CD69^+$ ) were further subgated on  $CD25^+Foxp3^+$  expression to evaluate the percentage of Tregs that comprise the total activated T cell population. Data are reported as mean±SD. \* $p < 0.05$ , \*\* $p < 0.01$  compared with PC. CSFE, carboxyfluorescein succinimidyl ester; NC, negative control; PC, positive control.



cell activation compared with the PC, the proportion of Tregs that comprised the activated T cell population was significantly lower across all three donors (figure 3D). On average, the maximum percentage of Tregs within the CD69<sup>+</sup> T cell population was twofold lower in TNB-585-treated cells compared with PC-treated cells, demonstrating preferential activation of effector T cells over Tregs by TNB-585.

### TNB-585 mediates robust killing of prostate tumor cells with reduced cytokine release

TNB-585-mediated tumor killing and cytokine release was evaluated in a co-culture assay using four PSMA<sup>+</sup> tumor cell lines (22Rv1, LNCaP, MDA-PCa-2b, and PC3-PSMA) incubated with resting T cells isolated from three healthy donors in the presence of TNB-585, PC, or NC. DU145 cells were used as an off-target, NC cell line. Tumor cell killing was assessed using either flow cytometry (22Rv1, MDA-PCa-2b, PC3-PSMA, and DU145) or WST-1 (LNCaP), and cytokine production was measured by MSD. TNB-585 mediated robust killing of all 4 PSMA<sup>+</sup> tumor cell lines with an average maximum tumor killing

of 60.1%–80.6% and EC<sub>50</sub> values ranging from 6.5 to 49.3 nM across the three donors (figure 4). In comparison with the PC, TNB-585 induced similar levels of maximum tumor killing but with substantially reduced cytokine release. At concentrations sufficient to induce maximum tumor killing, TNB-585 induced less IL-2, IL-6, IFN $\gamma$ , and TNF $\alpha$  production compared with the PC. No antibody-mediated tumor killing or cytokine release was observed in the presence of either DU145 cells or NC.

### TNB-585 demonstrates potent cytotoxicity of 3D tumor spheroids

Since TNB-585 is being developed for the treatment of a solid tumor, its efficacy was tested against 3D tumor spheroids to better represent the solid tumor setting and to allow for the analysis of T cell infiltration by IHC following treatment. Antitumor activity in a spheroid culture model was assessed by incubating LNCaP spheroids with healthy donor PBMCs at an E:T ratio of 1:1 in the presence of TNB-585, PC, or NC for 4 days at 37°C. As demonstrated in figure 5A, treatment with either TNB-585 or PC resulted in dissociation of spheroid integrity over

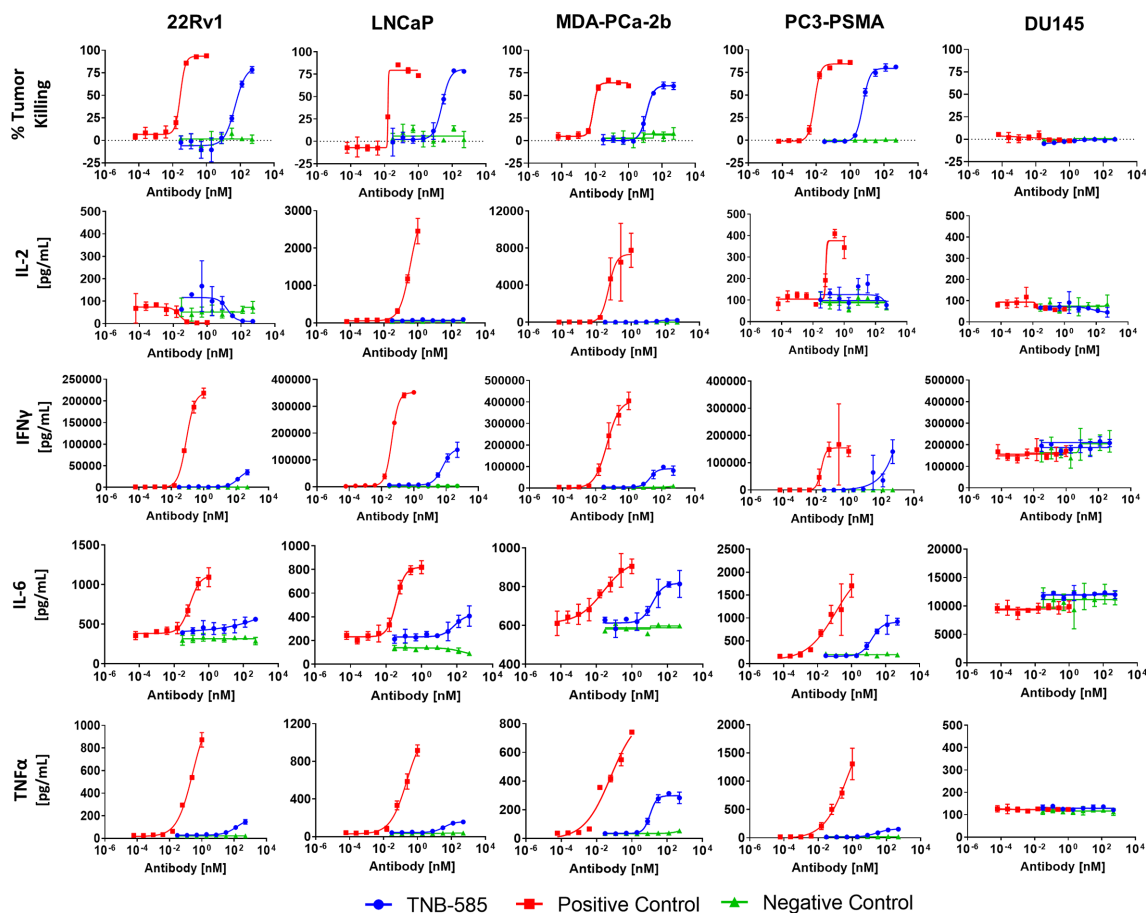


**Figure 4** TNB-585 induces tumor cell killing with reduced cytokine release. TNB-585 mediated tumor killing and cytokine release was evaluated against four PSMA<sup>+</sup> cell lines (22RV1, LNCaP, MDA-PCa-2b, and PC3-PSMA) and one PSMA<sup>-</sup> cell line (DU145) using T cells isolated from three healthy donors. T cells were incubated with prostate tumor cells at a 10:1 E:T ratio in the presence of increasing concentrations of TNB-585, PC, or NC. Cytotoxicity was measured using either WST-1 (LNCaP) or flow cytometry (22Rv1, MDA-PCa-2b, PC3-PSMA, and DU145). Cytokine (IL-2, IFN $\gamma$ , IL-6, and TNF $\alpha$ ) concentrations in culture supernatants were measured using MSD technology. Representative dose response curves from a single donor are shown. Data are reported as mean $\pm$ SD. NC, negative control; PC, positive control.

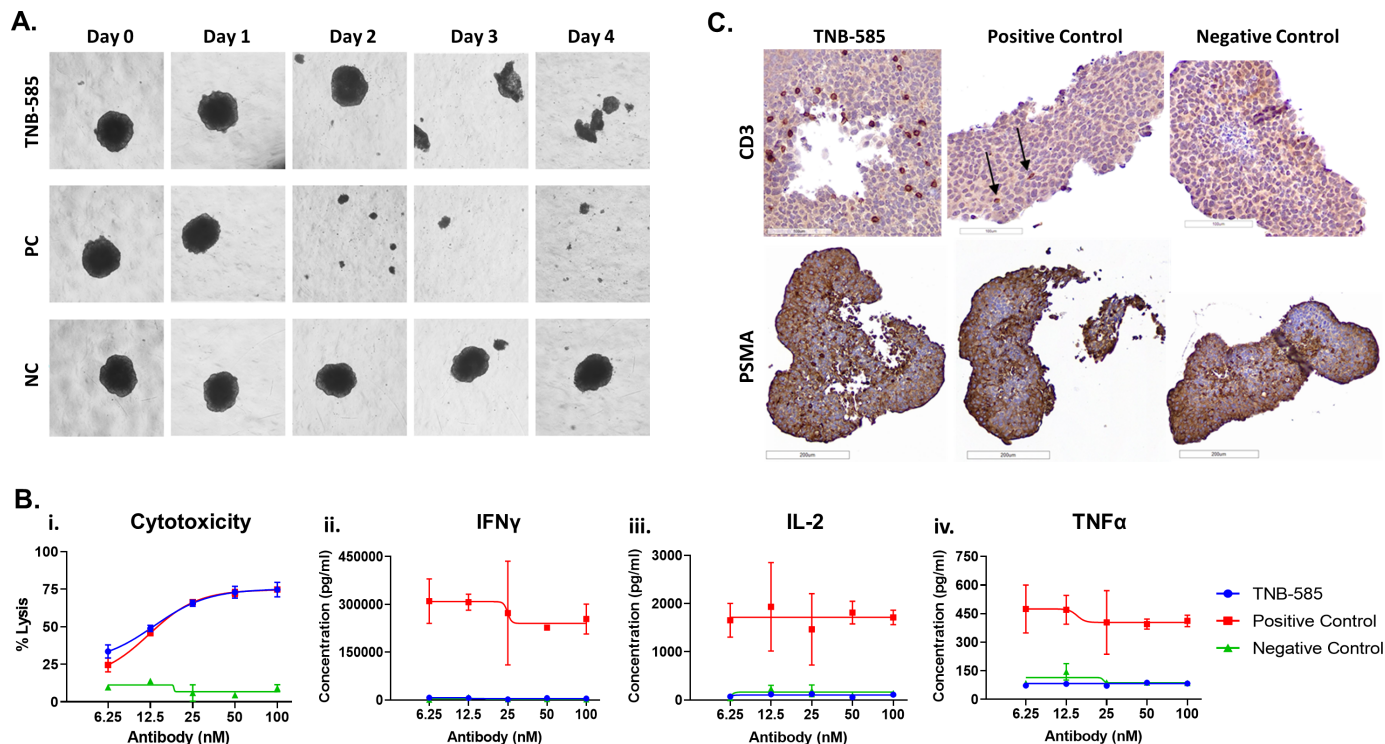


**Figure 5** TNB-585 mediates cytotoxicity of PSMA<sup>+</sup> LNCaP spheroids with minimal cytokine production. LNCaP spheroids were incubated with huPBMCs at an E:T ratio of 1+1 in the presence of increasing concentrations of TNB-585, PC, or NC for 4 days at 37°C. (A) Images were taken daily to capture morphological changes in the spheroids (100 nM antibody concentration is shown). Cytotoxicity (Bi) was assessed by LDH release, and cytokine concentrations (Bii–iv) were measured using MSD technology. (C) Spheroids were analyzed by IHC using anti-PSMA and anti-CD3 antibodies to evaluate T cell infiltration. Scale: top panel: 100  $\mu$ m; bottom panel: 200  $\mu$ m. IHC, Immunohistochemistry; LDH, lactate dehydrogenase; NC, negative control; PC, positive control.

time, while treatment with NC showed no difference in size after 4 days of treatment. TNB-585 induced dose-dependent killing of LNCaP spheroids (figure 5Bi) with minimal cytokine release (figure 5Bii, iii and iv). The maximum percent killing for TNB-585-treated and PC-treated cells were comparable at approximately 80%. However, the PC induced substantial secretion of IFN $\gamma$ , IL-2, and TNF $\alpha$ , while TNB-585 induced cytokine secretion at levels similar to the NC. Tumor killing was also assessed qualitatively by trypan blue staining. As seen in online supplemental figure S2, a higher staining intensity as well as significant morphological changes in terms of compromised tumor integrity were observed in TNB-585- and PC-treated spheroids compared with NC, indicating tumor death.

To assess T cell infiltration within the 3D tumors, IHC staining was performed. Representative IHC images shown in figure 5C demonstrate that TNB-585 induced CD3<sup>+</sup> T cell infiltration into the PSMA<sup>+</sup> LNCaP spheroids, whereas no T cell infiltration was observed in the NC-treated spheroids.

#### TNB-585 is efficacious against ex vivo patient prostate tumors

We analyzed five prostate patient tumor samples either freshly isolated (n=2) or previously frozen (n=3) for T cell mediated cytotoxicity and cytokine release by TNB-585. As shown in figure 6A, TNB-585 induced dose-dependent

killing of PSMA<sup>+</sup> tumor cells similar to PC, as measured by percent tumor cell death, in all tested conditions including freshly dissociated tumor incubated with TNB-585 in the absence of exogenous PBMCs (figure 6Ai and ii). While the PC induced substantial secretion of all cytokines tested, TNB-585 induced cytokine secretion comparable with the NC (figure 6B and online supplemental figure S3), correlating with our in vitro results.

#### TNB-585 induces immune cell infiltration and dose-dependent tumor regression in an NCG mouse xenograft model

The in vivo pharmacologic activity of TNB-585 was evaluated in NCG mouse xenograft models. In the first study, immunodeficient NCG mice were engrafted with C4-2 tumor cells and either resting T cells or preactivated PBMCs as indicated in the study design (figure 7A). Mice were administered (intravenous) TNB-585, PC, or NC biweekly at 150  $\mu$ g per dose, and tumor burden was monitored twice a week by measuring tumor volume. As demonstrated in figure 6B, TNB-585 and PC treatment resulted in comparable inhibition of tumor growth in both conditions whether resting T cells or preactivated PBMCs were used as effector cells. After termination of the in-life portion of the study, the tumors were harvested and stained using an anti-human CD45 antibody to visualize tumor infiltrating lymphocytes (TILs) by IHC. Greater immune cell (CD45<sup>+</sup>) infiltration of tumors in TNB-585

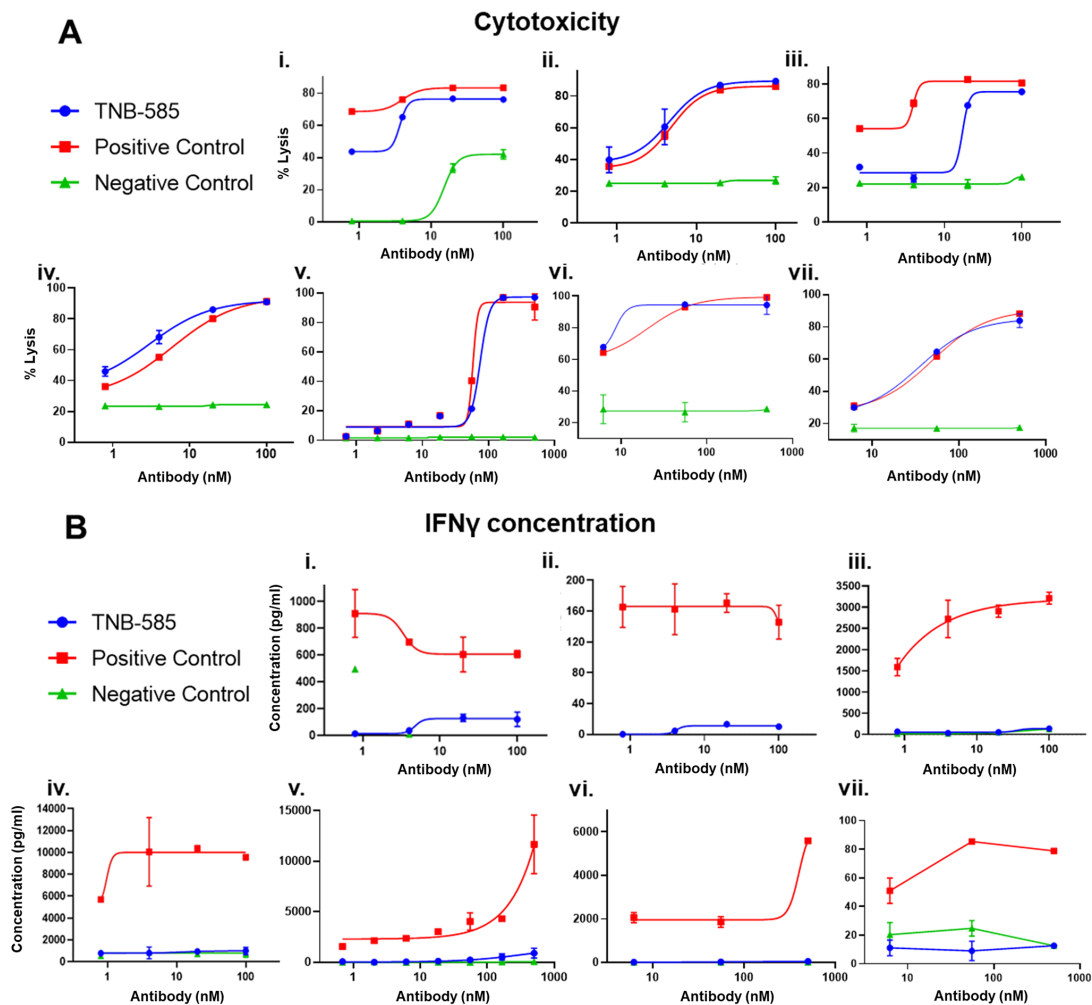


**Figure 6** TNB-585 mediates lysis of patient-derived prostate tumors with minimal cytokine production. TNB-585, PC, or NC were added to dissociated tumor cells from freshly procured prostatic adenocarcinoma tissue (i–iv) or thawed previously dissociated prostatic adenocarcinoma (v–vii) and incubated without additional human PBMCs (i, ii) or with either unmatched huPBMC (iii–iv) or donor matched huPBMC (v–vii) at an effector to target cell ratio (E:T=1:2) for 24 hours at 37°C and 8% CO<sub>2</sub>. Percent cytotoxicity of PSMA-positive cells (A) and IFN $\gamma$  concentration in the corresponding wells (B) are shown. NC, negative control; PBMCs, Peripheral blood mononuclear cells; PC, positive control.

treated and PC-treated mice was observed compared with tumors of NC-treated mice (online supplemental figure S4).

In a follow-on study, mice were administered preactivated PBMCs and treated biweekly with TNB-585 at doses ranging from 5.5  $\mu$ g to 450  $\mu$ g or vehicle. On day 28 post-implantation, the tumor growth inhibition was 27.8%, 87.4%, 98.4%, 99.2%, and 100% for dose groups 5.6, 16.7, 50, 150, and 450  $\mu$ g, respectively, demonstrating dose-dependent tumor regression by TNB-585 (figure 7Ci). An IHC analysis of the harvested tumors revealed substantial immune cell infiltration in tumors of TNB-585-treated mice, whereas the vehicle treated mice had no detectable TILs (figure 7Cii).

## DISCUSSION

TCEs are an emerging class of antibody-based immunotherapies that redirect the cytolytic activity of T cells to

kill cancer cells. Following the Food and drug administration (FDA) approval of blinatumomab in 2014, TCEs have gained momentum in cancer immunotherapy, and currently, there are 38 TCEs being investigated in clinical trials for patients with cancer.<sup>34</sup> Although T cell redirecting approaches are promising, treatment in the clinic has been hampered due to the toxicities associated with CRS, an acute systemic inflammatory condition triggered by elevated levels of proinflammatory cytokines. The immunosuppressive microenvironment of solid tumors presents additional challenges to the clinical success of TCEs, as the lack of effector T cell infiltration combined with an increased frequency of Tregs poses a significant barrier to efficacy against solid tumors.<sup>35</sup> To overcome these challenges, TNB-585 has been designed using a low-affinity anti-CD3 in order to induce tumor killing with reduced cytokine release, promote immune cell infiltration into tumors, and minimize Treg activation thereby

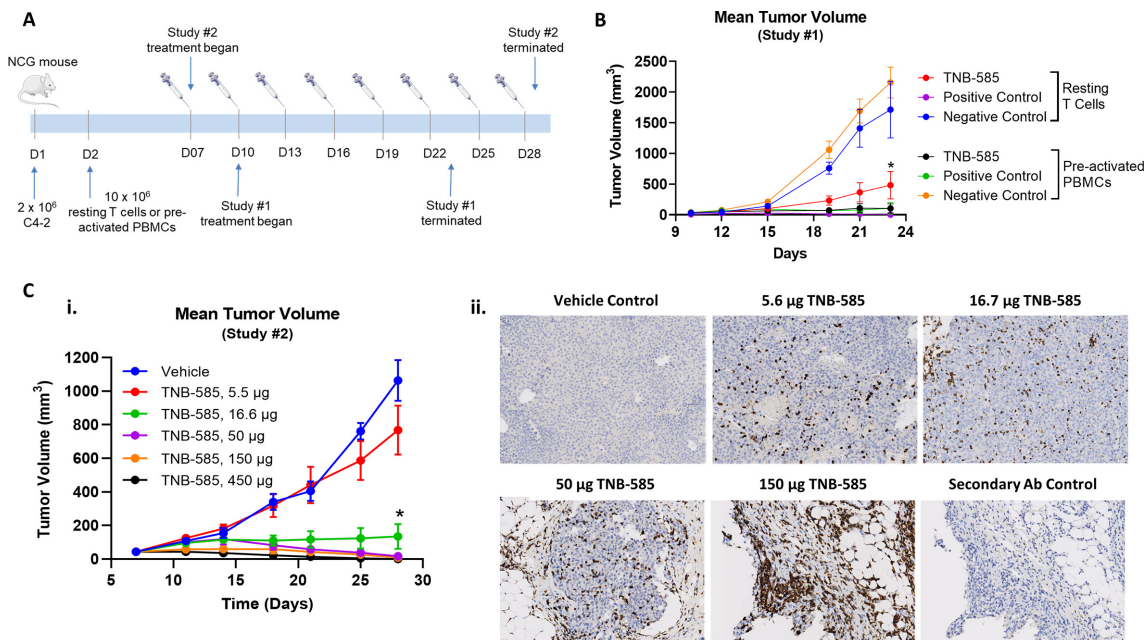


**Figure 7** TNB-585 induces immune cell infiltration and dose-dependent tumor regression in an NCG mouse xenograft model. (A) A schematic representation of the study designs is shown. NCG mice were engrafted with  $2 \times 10^6$  C4-2 tumor cells followed by injection of either resting T cells or preactivated PBMCs. Biweekly treatment began when the average tumor volume was  $\sim 50 \text{ mm}^3$ . (B) Tumor growth inhibition was evaluated in C4-2 tumor bearing mice comparing treatment with TNB-585, PC, and NC ( $150 \mu\text{g}/\text{dose}$ ) using either resting T cells or preactivated PBMCs as effectors cells. (C) Tumor growth inhibition was evaluated in C4-2 tumor bearing mice using preactivated PBMCs at TNB-585 doses ranging from 5.5 to  $450 \mu\text{g}$  per dose. tumor volumes were measured twice per week (i). At the end of study, tumors were harvested and stained by IHC using an anti-CD45 antibody to evaluate immune cell infiltration into the tumor. Representative images for each dose group are shown (ii). Tumor volumes are reported as mean  $\pm$  SEM. \* $P < 0.05$  compared with negative or vehicle treated control. NC, negative control; PC, positive control.

creating an efficacious therapeutic that reduces the potential for dose-limiting toxicities associated with CRS.

In the treatment of solid tumors, one major challenge is overcoming the lack of effector T cell infiltration in the tumor, leading to a non-inflamed or ‘cold’ state. Effector T cells play a key role in tumor immunity as studies have demonstrated a correlation between the presence of tumor infiltrating lymphocytes and progression-free survival.<sup>36</sup> In the mouse xenograft model described in the current study, an IHC analysis of the harvested tumors revealed that TNB-585 induced substantial immune cell infiltration into the tumor compared with vehicle-only treated mice. The significant tumor growth inhibition observed without preactivating the T cells demonstrated that TNB-585 is able to activate resting T cells in the presence of a PSMA<sup>+</sup> tumor in vivo. IHC of LNCaP 3D spheroids also showed CD3 T cell infiltration within the TNB-585 treated tumor. Furthermore, TNB-585 was shown to be effective at low E:T ratios, as demonstrated by ex vivo cytotoxicity assays in which potent killing of patient-derived prostate tumors was observed at 3% endogenous effector cells. The totality of these results suggests that TNB-585 promotes T cell infiltration into the prostate tumor bed and that this infiltration is sufficient to support antitumor activity, even when the number of available T cells is low. These findings are consistent with studies of T cell infiltration of tumors induced by other TCEs.<sup>37</sup>

Another obstacle of T cell engaging therapies in treating solid tumors is the presence of Tregs that contribute to an immunosuppressive microenvironment. Tregs, an immunosuppressive T cell subset, promote tumor progression by suppressing antitumor responses and promoting tolerance toward cancer cells.<sup>38</sup> Elevated numbers of Tregs in solid tumors is correlated with poor prognosis and lower overall survival.<sup>39</sup> In the current study, TNB-585 induced preferential activation of effector T cells over Tregs, as indicated by a significantly lower proportion of CD25<sup>+</sup>Foxp3<sup>+</sup> T cells that comprised the total CD69<sup>+</sup> T cell population compared with the PC. Differential activation through CD3 by low-affinity anti-CD3 binding arm may be the reason for this,<sup>40</sup> which could provide an invaluable benefit in targeting tumor cells in a solid tumor microenvironment.

Lastly, TCEs are designed to activate T cells and redirect their cytolytic activity to tumor cells, but this immune activation has the potential to lead to toxic adverse events including CRS, which is characterized by the systemic release of proinflammatory cytokines, causing symptoms such as fever, headache, and nausea and in serious cases organ failure and death.<sup>41</sup> To address this concern, we developed a low-affinity anti-CD3 (CD3\_F2B) that enables tumor killing with low cytokine release in order to reduce the risk of CRS while maintaining maximum efficacy. Safety and efficacy of CD3\_F2B has been validated in the

clinic for the treatment of MM using TNB-383B, our anti-BCMA $\times$ CD3 TCE.<sup>42</sup> By incorporating the same anti-CD3<sub>F2B</sub>, TNB-585 induced maximal killing of prostate tumor cells with reduced cytokine release compared with the PC in all preclinical studies tested, suggesting that TNB-585 may be efficacious while inducing a lower incidence and severity of CRS in CaP patients compared with other TCEs that incorporate high-affinity anti-CD3s.

## CONCLUSION

In summary, TNB-585 is a novel CD3 $\times$ PSMA TCE in development for the treatment of mCRPC that warrants further investigation in clinical trials. Our data demonstrate that TNB-585 induces antigen-dependent and dose-dependent killing of PSMA<sup>+</sup> tumor cells in vitro (2D cultures and 3D spheroids), ex vivo, and in vivo. In all preclinical models tested, TNB-585 stimulated significantly less cytokine production compared with a PC antibody that contains the same anti-PSMA arm but a higher affinity anti-CD3 arm. Our results suggest that TNB-585, with its low-affinity anti-CD3, may provide an efficacious approach to kill PSMA<sup>+</sup> CaP cells while inducing a lower incidence and severity of CRS in patients.

**Acknowledgements** The authors would like to thank Heather Ogana for her contributions during the primary and diversity screens of the anti-PSMA antibody discovery phase.

**Contributors** KD, PD, GC, SI, and YL contributed to manuscript preparation. KD, PD, GC, YL, and SCC contributed to the study design and analysis of results. NDT, KEH, and AB performed the NGS-based repertoire analysis. KEH, LMD, and AB completed the molecular biology. KD, SCC, and PS performed the ELISA and flow cytometry lead discovery assays. DP characterized the anti-CD3 antibodies. YL and HSU conducted the expression, purification, and biophysical characterization of antibodies. WS contributed to the developability assessment. KD, PD, and GC performed the in vitro functional assays. PD, KD, BB, and SCC contributed to the in vivo study designs. RD performed the cynomolgus PK analysis. AS, SK and LF provided the fresh patient tumors for ex vivo analysis. PD designed and performed the ex vivo assays. SI, BB, US, WvS, and RB contributed to overall data review. All authors reviewed and approved the final manuscript.

**Funding** The study was sponsored by Teneobio, Inc and funded in part by SBIR grant number 1R43CA232972-01 awarded to Teneobio, Inc. LF's lab is separately funded by the Prostate Cancer Foundation Challenge Grant and NIH R01CA223484.

**Competing interests** All authors except AS, SK, and LF were employees of Teneobio, Inc with equity interests when the reported work was conducted. LF and RD are consultants of Teneobio, Inc.

**Patient consent for publication** Not required.

**Ethics approval** Human PBMCs were collected by STEMCELL Technologies and AllCells in accordance with scientific, ethical, and regulatory guidelines. Rat maintenance and immunizations were performed by Antibody Solutions (Sunnyvale, California, USA) with protocols reviewed by Institutional Animal Care and Use Committee (IACUC) boards. Mouse studies were reviewed and approved by the IACUC of CrownBio prior to execution, and studies were conducted in accordance with the regulations of the Association for Assessment and Accreditation of Laboratory Animal Care.

**Provenance and peer review** Not commissioned; externally peer reviewed.

**Data availability statement** All data relevant to the study are included in the article or uploaded as supplementary information. All data relevant to the study are included in the article or uploaded as supplementary information.

**Supplemental material** This content has been supplied by the author(s). It has not been vetted by BMJ Publishing Group Limited (BMJ) and may not have been peer-reviewed. Any opinions or recommendations discussed are solely those of the author(s) and are not endorsed by BMJ. BMJ disclaims all liability and

responsibility arising from any reliance placed on the content. Where the content includes any translated material, BMJ does not warrant the accuracy and reliability of the translations (including but not limited to local regulations, clinical guidelines, terminology, drug names and drug dosages), and is not responsible for any error and/or omissions arising from translation and adaptation or otherwise.

**Open access** This is an open access article distributed in accordance with the Creative Commons Attribution Non Commercial (CC BY-NC 4.0) license, which permits others to distribute, remix, adapt, build upon this work non-commercially, and license their derivative works on different terms, provided the original work is properly cited, appropriate credit is given, any changes made indicated, and the use is non-commercial. See <http://creativecommons.org/licenses/by-nc/4.0/>.

## ORCID iDs

Kevin Dang <http://orcid.org/0000-0001-5695-926X>

Giulia Castello <http://orcid.org/0000-0002-5647-178X>

Pranjali Dalvi <http://orcid.org/0000-0002-5247-9645>

## REFERENCES

- 1 Rawla P. Epidemiology of prostate cancer. *World J Oncol* 2019;10:63–89.
- 2 National Cancer Institute. Seer cancer STAT facts: prostate cancer. Available: <https://seer.cancer.gov/statfacts/html/prost.html>
- 3 Patrikidou A, Loriot Y, Eymard J-C, et al. Who dies from prostate cancer? *Prostate Cancer Prostatic Dis* 2014;17:348–52.
- 4 Karantanos T, Evans CP, Tombal B, et al. Understanding the mechanisms of androgen deprivation resistance in prostate cancer at the molecular level. *Eur Urol* 2015;67:470–9.
- 5 Teo MY, Rathkopf DE, Kantoff P. Treatment of advanced prostate cancer. *Annu Rev Med* 2019;70:479–99.
- 6 Chang SS. Overview of prostate-specific membrane antigen. *Rev Urol* 2004;6 Suppl 10:S13–18.
- 7 Kiessling A, Wehner R, Füssel S, et al. Tumor-Associated antigens for specific immunotherapy of prostate cancer. *Cancers* 2012;4:193–217.
- 8 Caromile LA, Dortche K, Rahman MM, et al. Psma redirects cell survival signaling from the MAPK to the PI3K-Akt pathways to promote the progression of prostate cancer. *Sci Signal* 2017;10. doi:10.1126/scisignal.aag3326. [Epub ahead of print: 14 Mar 2017].
- 9 Kawakami M, Nakayama J. Enhanced expression of prostate-specific membrane antigen gene in prostate cancer as revealed by in situ hybridization. *Cancer Res* 1997;57:2321–4.
- 10 Silver DA, Pellicer I, Fair WR, et al. Prostate-Specific membrane antigen expression in normal and malignant human tissues. *Clin Cancer Res* 1997;3:81–5.
- 11 Mhawech-Fauceglia P, Zhang S, Terracciano L, et al. Prostate-Specific membrane antigen (PSMA) protein expression in normal and neoplastic tissues and its sensitivity and specificity in prostate adenocarcinoma: an immunohistochemical study using multiple tumour tissue microarray technique. *Histopathology* 2007;50:472–83.
- 12 Hupe MC, Philippi C, Roth D, et al. Expression of prostate-specific membrane antigen (PSMA) on biopsies is an independent risk stratifier of prostate cancer patients at time of initial diagnosis. *Front Oncol* 2018;8:623.
- 13 Bravaccini S, Puccetti M, Bocchini M, et al. Psma expression: a potential ally for the pathologist in prostate cancer diagnosis. *Sci Rep* 2018;8:4254.
- 14 Kaittanis C, Andreou C, Hieronymus H, et al. Prostate-Specific membrane antigen cleavage of vitamin B9 stimulates oncogenic signaling through metabotropic glutamate receptors. *J Exp Med* 2018;215:159–75.
- 15 Marshall CH, Antonarakis ES. Emerging treatments for metastatic castration-resistant prostate cancer: immunotherapy, PARP inhibitors, and PSMA-targeted approaches. *Cancer Treat Res Commun* 2020;23:100164.
- 16 Sedykh SE, Prinz VV, Buneva VN, et al. Bispecific antibodies: design, therapy, perspectives. *Drug Des Devel Ther* 2018;12:195–208.
- 17 Wu Z, Cheung NV. T cell engaging bispecific antibody (T-BsAb): from technology to therapeutics. *Pharmacol Ther* 2018;182:161–75.
- 18 Cruz E, Kayser V. Monoclonal antibody therapy of solid tumors: clinical limitations and novel strategies to enhance treatment efficacy. *Biologicals* 2019;13:33–51.
- 19 Cha H-R, Lee JH, Ponnazhagan S. Revisiting immunotherapy: a focus on prostate cancer. *Cancer Res* 2020;80:1615–23.
- 20 Hummel H-D, Kufer P, Grülllich C, et al. Pasotuxizumab, a BiTE<sup>®</sup> immune therapy for castration-resistant prostate cancer: Phase I, dose-escalation study findings. *Immunotherapy* 2021;13:125–41.



- 21 Tran B, Horvath L, Dorff TB, *et al.* Phase I study of AMG 160, a half-life extended bispecific T-cell engager (HLE bite) immune therapy targeting prostate-specific membrane antigen (PSMA), in patients with metastatic castration-resistant prostate cancer (mCRPC). *JCO* 2020;38:TPS261
- 22 Bendell JC, Fong L, Stein MN, *et al.* First-In-Human phase I study of HPN424, a tri-specific half-life extended PSMA-targeting T-cell engager in patients with metastatic castration-resistant prostate cancer (mCRPC). *JCO* 2020;38:5552
- 23 Faroudi M, Utny C, Salio M, *et al.* Lytic versus stimulatory synapse in cytotoxic T lymphocyte/target cell interaction: manifestation of a dual activation threshold. *Proc Natl Acad Sci U S A* 2003;100:14145–50.
- 24 Purbhoo MA, Irvine DJ, Huppa JB, *et al.* T cell killing does not require the formation of a stable mature immunological synapse. *Nat Immunol* 2004;5:524–30.
- 25 Trinklein ND, Pham D, Schellenberger U, *et al.* Efficient tumor killing and minimal cytokine release with novel T-cell agonist bispecific antibodies. *MAbs* 2019;11:639–52.
- 26 Malik-Chaudhry HK, Ugamraj HS, Boudreau A, *et al.* TNB-486 induces potent tumor cytotoxicity coupled with low cytokine release in preclinical models of B-NHL. *MAbs*, 2021.
- 27 Harris KE, Aldred SF, Davison LM, *et al.* Sequence-Based discovery demonstrates that fixed light chain human transgenic rats produce a diverse repertoire of antigen-specific antibodies. *Front Immunol* 2018;9:889.
- 28 Clarke SC, Ma B, Trinklein ND, *et al.* Multispecific antibody development platform based on human heavy chain antibodies. *Front Immunol* 2018;9:3037.
- 29 Ridgway JB, Presta LG, Carter P. 'Knobs-into-holes' engineering of antibody CH3 domains for heavy chain heterodimerization. *Protein Eng* 1996;9:617–21.
- 30 Canfield SM, Morrison SL. The binding affinity of human IgG for its high affinity Fc receptor is determined by multiple amino acids in the CH2 domain and is modulated by the hinge region. *J Exp Med* 1991;173:1483–91.
- 31 Strand DW, Aaron L, Henry G, *et al.* Isolation and analysis of discreet human prostate cellular populations. *Differentiation* 2016;91:139–51.
- 32 Carlin S, Zhang H, Tandon N. Quantification of PSMA expression in primary human and xenograft tumors using radioligand binding and digital autoradiography. *J Nucl Med* 2015;56:68
- 33 Trapani JA, Smyth MJ. Functional significance of the perforin/granzyme cell death pathway. *Nat Rev Immunol* 2002;2:735–47.
- 34 Suurs FV, Lub-de Hooge MN, de Vries EGE, *et al.* A review of bispecific antibodies and antibody constructs in oncology and clinical challenges. *Pharmacol Ther* 2019;201:103–19.
- 35 Beyer M, Schultze JL. Regulatory T cells in cancer. *Blood* 2006;108:804–11.
- 36 Zhang J, Endres S, Kobold S. Enhancing tumor T cell infiltration to enable cancer immunotherapy. *Immunotherapy* 2019;11:201–13.
- 37 Staffin K, Zuch de Zafra CL, Schutt LK, *et al.* Target arm affinities determine preclinical efficacy and safety of anti-HER2/CD3 bispecific antibody. *JCI Insight* 2020;5. doi:10.1172/jci.insight.133757. [Epub ahead of print: 09 Apr 2020].
- 38 Facciabene A, Motz GT, Coukos G. T-Regulatory cells: key players in tumor immune escape and angiogenesis. *Cancer Res* 2012;72:2162–71.
- 39 Saleh R, Elkord E. FoxP3<sup>+</sup> T regulatory cells in cancer: Prognostic biomarkers and therapeutic targets. *Cancer Lett* 2020;490:174–85.
- 40 Poltorak MP, Graef P, Tschulik C, *et al.* Expamers: a new technology to control T cell activation. *Sci Rep* 2020;10:17832.
- 41 Trabolsi A, Arumov A, Schatz JH. T cell-activating bispecific antibodies in cancer therapy. *J Immunol* 2019;203:585–92.
- 42 Rodriguez C. *Initial results of a phase I study of TNB-383B, a BCMA X CD3 bispecific T-cell Redirecting antibody in relapsed/refractory multiple myeloma. in ash*, 2020.